

Abstract

Rising sea levels, subsidence, and decreased fluvial sediment load threaten river deltas and their marshes. However, the feedbacks between fluvial and marsh deposition remain weakly constrained. We investigate how marsh accumulation impacts the fluvial sediment partitioning between a delta's topset, coastal zone, and foreset by comparing a delta experiment with proxy marsh accumulation to a control. Marsh accumulation alters fluvial sediment distribution by decreasing the slope in the subaerial marsh window by $\sim 40\%$, creating an $\sim 8\%$ larger delta top and a $\sim 100\%$ larger marsh platform. The reduced slopes decrease relative delta elevation, and fluvial incursions into the marsh trap 1.3 times more clastic volume. The volume exported to deep water remains unchanged. Marsh deposition shifts elevation distributions towards sea level, which produces a hypsometry akin to field-scale deltas. Given that risk is tied to elevation, marsh accumulation accentuates low-elevation areas, while providing essential land-building capabilities.

Plain Language Summary

Low-lying deltaic coastal zones, often with abundant vegetation (wetlands), are threatened worldwide because of rising sea level and decreased sediment supply of large rivers flowing to coastal regions. The accumulation of sediment in low-lying coastal areas is a fundamental process that helps these regions keep pace with rising sea level. This sediment may be delivered from rivers that deposit their sediment when they reach the coast, from off-shore through tides and waves, and/or through the production of plant material. Our study shows that sediment accumulated in coastal wetlands alters the elevation distribution of coastal regions and the spatial deposition of the river sediment. These results provide important information for future plans to help regain coastal land area.

1 Introduction

River deltas and their marsh platforms are diverse ecosystems threatened by anthropogenic impacts to coastal areas, such as rising sea levels, subsidence, and leveeing of channels (Ericson et al., 2006). Organic material production, a critical form of sediment accumulation in many river deltas, is the primary driver of marsh platform growth (Nyman et al., 2006), whereas clastic sedimentation via rivers drives deltaic lobe growth (Edmonds et al., 2009). To successfully predict the long-term fate of these ecosystems, the interaction controlling delta and marsh growth must be understood (Paola et al., 2011). While much is known about surface processes in channelized portions of river deltas (Edmonds & Slingerland, 2008; Q. Li et al., 2017; Smart & Moruzzi, 1971) and much is known about sediment accumulation in marshes (Allen, 2000; Kirwan & Murray, 2007; Morris et al., 2002), the manner in which they interact remains largely uninvestigated.

Aerial imagery and the stratigraphic record show evidence of delta-marsh interaction in modern and ancient systems, and it is well known that deltaic channel deposits are sensitive to the deposition of fine-grained and organic material in floodplains (Bohacs & Suter, 1997; Esposito et al., 2017; Hoyal & Sheets, 2009). For example, $\sim 25\%$ of the recent Mississippi River Delta sedimentation was organic marsh material (by mass) (Holmquist et al., 2018; Sanks et al., 2020). Further, evidence preserved in strata suggests organic-rich deposition influenced deltaic processes over most of the Phanerozoic (Chesnut & Greb, 1992). Both modern and ancient records suggest that clastic inputs influence the stability and growth of the marsh platform, thus influencing coastal sustainability.

Previous experimental and numerical studies have added cohesion to show that vegetation influences river deltas (Hoyal & Sheets, 2009; Q. Li et al., 2017). While increased cohesion was necessary to understand the evolution of deltaic systems, a key component of deltaic sediment accumulation is neglected from these previous studies: marsh sediment accumulation. This sediment accumulates in low-lying regions of deltas worldwide

69 and supplements clastic deposition. Marsh sediment includes both mineral and organic
 70 sediment (Sanks et al., 2020). The organic component is formed in-situ via primary pro-
 71 duction of plants and accumulates as a parabolic function of elevation relative to sea level,
 72 with maximum production occurring around mean high tide (Morris et al., 2002).

73 Here, we investigate the influence of marsh accumulation on delta morphology and
 74 mass balance by comparing two physical experiments conducted at the Tulane Univer-
 75 sity Sediment Dynamics Laboratory. We incorporate proxy-marsh sediment accumula-
 76 tion in an experimental river delta, an important advance in experimental sedimentol-
 77 ogy and delta restoration. We compare this experiment to a previous, identical exper-
 78 iment that formed without marsh sedimentation. This setup is ideal to understand the
 79 interaction of ecogeomorphic processes in coastal marshes and physical processes of river
 80 deltas due to the ability to assess long-term behavior at reduced time and length scales,
 81 control on forcing conditions (supporting information, Table 1), precise measurements,
 82 and autogenic dynamics (Paola et al., 2009). By analyzing the experiments over long timescales
 83 relative to autogenic dynamics, we can interpret any differences as direct results of marsh
 84 deposition.

85 2 Materials and Methods

86 2.1 Experimental Setup and Data

87 We investigate two experimental deltas formed under identical boundary conditions.
 88 The only difference is that the control experiment evolved without explicit marsh sed-
 89 imentation, while the treatment experiment evolved with the presence of marsh sedimen-
 90 tation (supporting information, Table 1). Both experiments were run for 560 hours (~ 10
 91 times the compensation timescale), which captures many channel avulsions and inher-
 92 ent stochasticity of the system (Straub et al., 2009). LiDAR scans of the basin were col-
 93 lected every one (control) or two (treatment) hours while the experiments were paused.
 94 Aerial imagery was taken every 15 minutes.

95 The deposit was sectioned from distal to proximal along strike every 10 cm. We
 96 use image processing to obtain a stratigraphic marsh fraction roughly every 10 cm in strike
 97 (supporting information, Figure 1), which was interpolated across the basin using Bayesian
 98 kriging techniques to estimate the marsh and clastic volume sequestered in the basin (sup-
 99 porting information).

100 2.2 Marsh Proxy

101 We use a physical delta experiment coupled with simulated organic material pro-
 102 duction (marsh proxy) to understand the interactions of river deltas and their marsh plat-
 103 forms (Figure 1a). For simplicity, the marsh proxy simulated only the sediment prop-
 104 erties of organic material, neglecting some physical properties of vegetation (e.g., stem
 105 density). We use kaolinite (clay) as the marsh proxy, which has a low initial bulk den-
 106 sity ($\sim 90\%$ porosity when deposited in water), uniform deposition upon settling, and rel-
 107 atively high settling velocity when surfactant (Jet Dry) is mixed into the water. Further,
 108 a distinctly different grain size and color from the riverine sediment makes it ideal to an-
 109alyze in aerial imagery (Figure 1a) and stratigraphy. Note that while we discuss this proxy
 110 in terms of organic sedimentation, it may also represent fine-grained deposition deposited
 111 via non-riverine processes (e.g., tides, waves, and storms) in tidal flats and wetland plat-
 112 forms. Thus, representing any elevation-based, non-riverine coastal accumulation.

113 To first order, marshes accumulate as a function of elevation relative to sea level
 114 (rsl) (Morris et al., 2002; Cahoon et al., 1995; Baustian et al., 2012; Kirwan et al., 2010).
 115 This generalization simplifies many complex processes of marsh ecology (Morris et al.,
 116 2002) and trapping of fine sediment (S. Li et al., 2009), yet the vast swaths of coastal

117 marsh within decimeters of sea level show that this is a dominant, emergent control. We
 118 simplify the marsh production model from Morris et al. (2002), which shows an optimum
 119 accumulation rate near mean water levels and suboptimal accumulation above and be-
 120 low. The experimental system was scaled to the emergent channel depth (~ 14 mm). Hence,
 121 generating three elevation zones that received marsh: -9 to -5 mm rsl (unstable), -5 to
 122 0 mm rsl (maximum production), and 0 to 5 mm rsl (stable), and collectively represent
 123 the marsh window. The maximum production zone received enough kaolinite to accu-
 124 mulate ~ 1 times the base relative sea level rise rate (RSLR_b; 0.5 mm/2-hrs). The un-
 125 stable and stable zones received enough sediment to accumulate ~ 0.5 RSLR_b (Figure 1b).

126 LiDAR scans taken while the experiment was paused provide median elevation of
 127 146.14 cm² hexagonal grid cells (7.5 cm sides), which determine the marsh window (Fig-
 128 ure 1c). If the median elevation of a hexagonal bin falls in the marsh zone, we deposit
 129 either 3.4 g (maximum production zone) or 1.7 g (stable and unstable zones) of kaoli-
 130 nite. The marsh sediment dispenser (a sieve) is attached to a cart that moves about the
 131 basin. Deposition is promoted by using a ButtKickerTM to vibrate the sieve (black box
 132 left of sieve in Figure 1a), triggering kaolinite to rain down on the delta top. On aver-
 133 age, we deposit the marsh proxy with $\sim 50\%$ accuracy (Figure 1d; ~ 60 g/hr less than
 134 the modeled rate). While less accurate than anticipated, in-situ deposition of kaolinite
 135 still provides a reasonable proxy for marsh accumulation, as shown by significantly al-
 136 tered morphology and clastic deposition in the treatment experiment compared to the
 137 control.

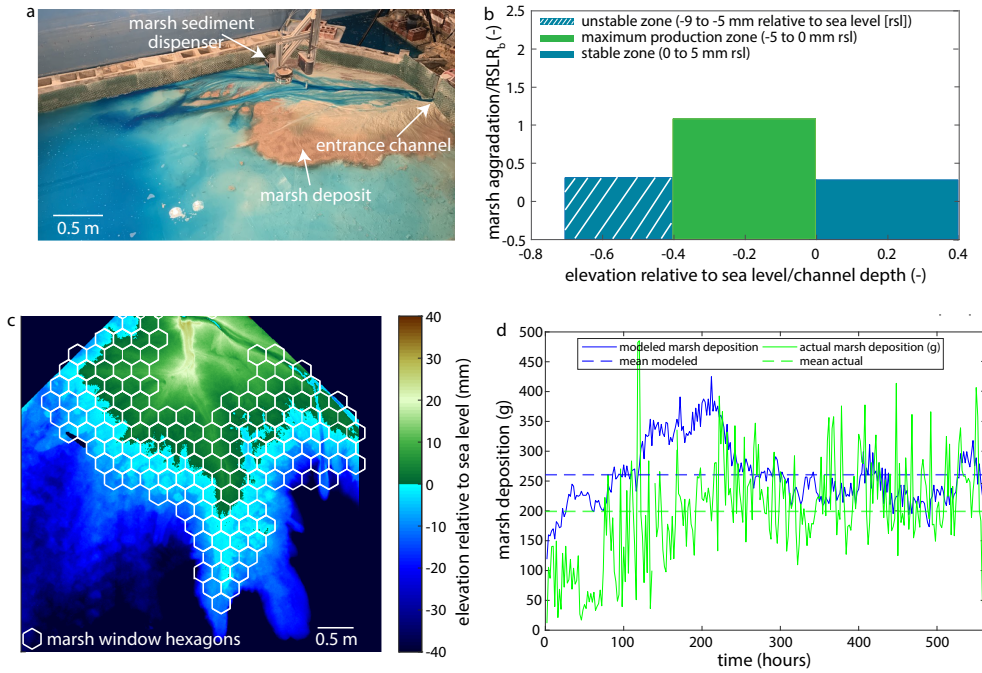


Figure 1: (a) The silver cart (top of image) holds the marsh sediment dispenser, which deposits kaolinite at the center of each hexagonal grid (c) with an average elevation in the marsh window every two hours. The brown sediment is the kaolinite marsh proxy. (b) The model, adapted from Morris et al. (2002), used to determine the marsh zone. (c) The hexagonal grid imposed upon a LiDAR scan of the basin (hour 250). (d) The modeled vs. actual marsh deposition (g) each hour during the experiment.

3 Results

3.1 Delta Morphology

A significant difference between treatment and control is observed in the area within the marsh window (5 to -9 mm rsl) and the total delta top (≥ -9 mm rsl). The marsh window was 0.936 ± 0.202 m² in the control, but larger in the treatment at an average size of 1.67 ± 0.288 m² (Figure 2a). Similarly, the delta top was smaller in the control at an average size of 2.80 ± 0.383 compared to 3.08 ± 0.316 m² for the treatment (Figure 2a). Considering the average delta top area, the treatment experiment was 10% larger than the control experiment, while the treatment marsh window was 78% larger.

The elevation distribution shows an increase in elevations within the marsh window in the treatment experiment (Figure 2b), suggesting a change in slope relative to the control. We measure slopes above the marsh window and in the subaerial marsh window radially from the apex, and observe no change in slope above the marsh ($\sim 3.0\%$ in both experiments). Interestingly, the slope in the sub-aerial marsh window (0 to 5 mm rsl to ensure no subaqueous distortion) is significantly reduced from 3.2% in the control to 2.4% in the treatment experiment (Figure 2c).

The mean elevation as a function of radial distance from the entrance channel shows that the addition of the marsh proxy alters the elevation distribution of the delta top (Figure 2d). The treatment experiment has an increase in marsh window elevations and a decrease in the area of elevations above the marsh window. The relative elevations above the marsh window are also smaller (by about one channel depth on average). Further, the delta top slope decreases upon entrance to the marsh window in the treatment, which allows the marsh to persist over a greater distance.

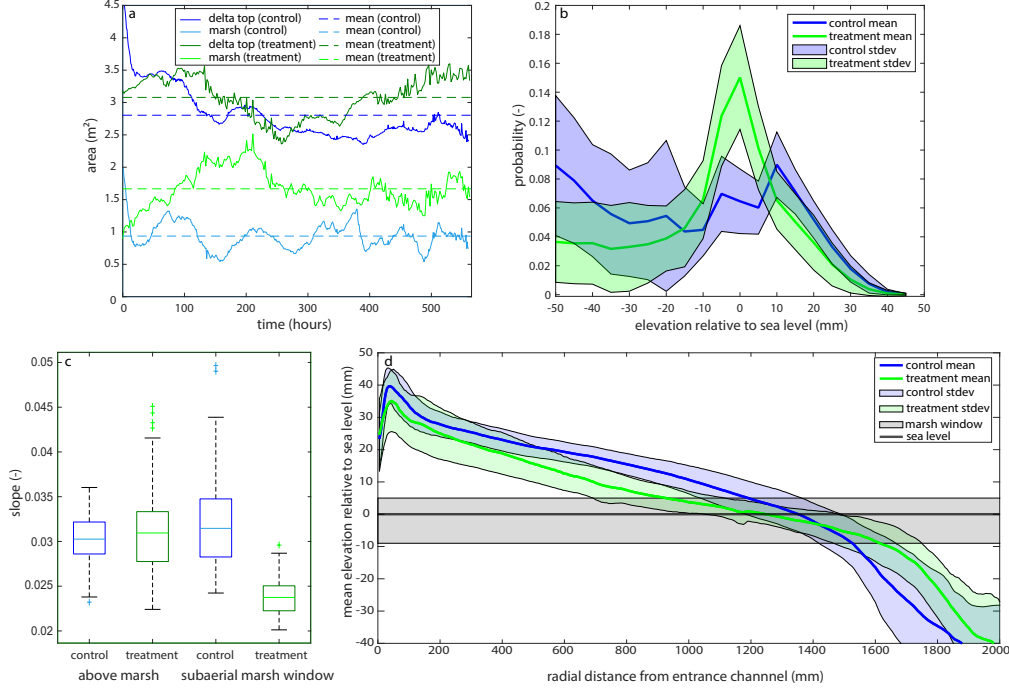


Figure 2: (a) Delta top (≥ -9 mm rsl) and marsh window (-9 to 5 mm rsl) area for the control and treatment through time. (b) Time-integrated mean probability distribution of elevations relative to sea level, with one standard deviation shown for both experiments. (c) Box plots showing the time distribution of above marsh and subaerial marsh window delta slopes. (d) Mean elevation (mm) as a function of radial distance from the entrance channel (mm) integrated over space and time, with one standard deviation shown for both experiments.

161

3.2 Sediment Balance

162

163

164

165

166

167

168

169

170

171

172

173

174

175

176

While each experiment had the same clastic sediment input, the spatial distribution of sediment accumulation is different (Figure 3). For volume balance and trapping efficiency equations refer to supporting information section 2.2. We compare the area that is above the marsh window for at least 90% of the experiment to the area that is in the marsh window for less than 10% of the experiment. We choose these two zones for comparison to limit delta-marsh interaction above the marsh window and compare two distinct areas with no overlap. The area above the marsh window for greater than 90% of the control experiment is 0.880 m^2 , which accumulates 0.121 m^3 of sediment throughout the experiment (Figure 3a; yellow area). The corresponding area of the treatment experiment is 0.352 m^2 , which accumulates 0.0413 m^3 of clastic sediment during the experiment (Figure 3b; yellow area). Since the marsh extent is larger in the treatment experiment (Figure 3a and b; turquoise area), more clastic sediment is trapped in this elevation window than in the control. Thus, the marsh window has a 68.6% trapping efficiency (clastic sediment delivered to the delta top/clastic sediment accumulated in marsh) in the treatment, but a 51.4% trapping efficiency in the control (Table 1).

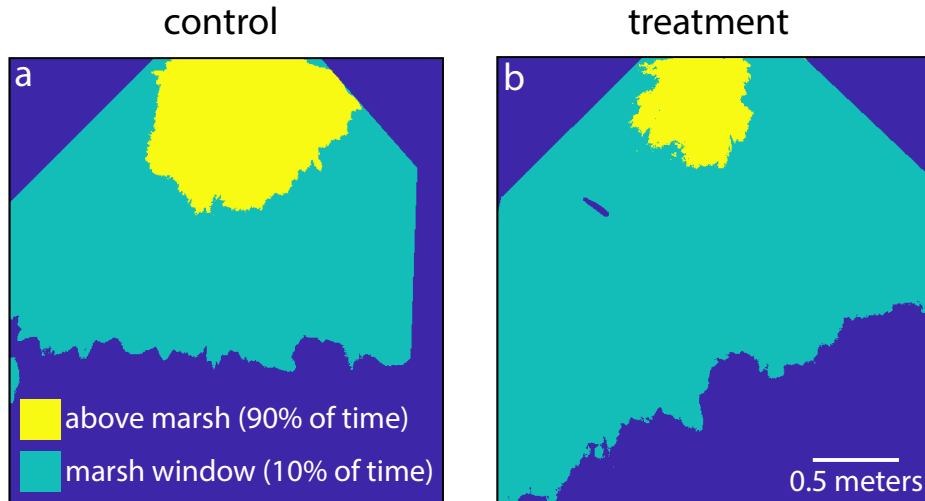


Figure 3: (a and b) The yellow area represents the area above 5 mm (above the marsh) for at least 90% of the (a) control and (b) treatment experiments, while the turquoise area represents the area in the marsh window (-9 to 5 mm) for greater than 10% of the experiment.

177 The area on the delta top (≥ -9 mm rsl) for at least 50% of the control experiment
 178 is 2.73 m^2 , accumulating a total volume of 0.363 m^3 of sediment. The corresponding area
 179 of the treatment experiment is slightly larger (2.96 m^2), but accumulates a less clastic
 180 sediment (0.355 m^3). The delta top area is smaller than the combined area shown in Fig-
 181 ure 3, as the relative time on the delta top ($\geq 50\%$ of experiment) and marsh window ($>10\%$
 182 of experiment) are different. We make this distinction here to compare average delta top
 183 conditions between the two experiments. Compared to the total fluvial input (0.660 m^3),
 184 this yields similar delta top trapping efficiencies of 55.0% in the control and 53.7% in the
 185 treatment (Table 1). Hence, similar amounts of clastic sediment are transported past the
 186 marsh zone. We also find that roughly 85% of the marsh deposited was preserved in the
 187 resulting delta top stratigraphy, which accounts for 15% of the delta top volume. Though
 188 the total clastic sediment sequestered here is similar in both experiments, marsh sed-
 189 imentation augments the clastic sedimentation in the treatment experiment leading to
 190 the formation of a vastly different delta.

Table 1: The clastic volume balance and trapping efficiency of different delta regions for the control and treatment experiments. Note that treatment marsh sedimentation is excluded.

Delta Region	Clastic volume (m ³) [control]	Clastic volume (m ³) [treatment]	Trapping efficiency (%) [control]	Trapping efficiency (%) [treatment]
delta top (\geq -9 mm rsl; 50% of time)	0.363	0.355	55.0	53.7
above marsh ($>$ 5 mm rsl; 90% of time)	0.121	0.0413	18.3	6.25
marsh window (-9 to 5 mm rsl; 10% of time)	0.339	0.453	51.4 [63.9 ^a]	68.6 [73.2 ^a]
off shore ($<$ -9 mm rsl; 50% of time)	0.297	0.306	100	100

^aThe trapping efficiency calculated using the volume of clastic sediment delivered to the marsh window instead of the clastic sediment delivered to the delta top. Refer to supporting information section 2.2 for equations and explanation related to this difference.

191 4 Discussion

192 The experiments show that marshes interact with deltas and have first-order im-
 193 pacts on morphology and sediment partitioning. We show that even a small addition of
 194 marsh proxy sediment (\sim 8% of riverine mass) drastically impacts delta formation. Specif-
 195 ically, marsh deposition flattens the delta, alters location of maximum clastic deposition,
 196 and changes the delta hypsometry.

197 4.1 An important feedback

198 It is remarkable that an 8% addition of marsh mass creates a \sim 100% increase in
 199 extent of the marsh window. This marsh sedimentation is essential to the long-term sta-
 200 bility of the treatment experiment. Paradoxically, the addition of marsh proxy reduces
 201 total clastic sedimentation on the delta top, but simultaneously bridges the gap to cre-
 202 ate a delta spanning a similar extent. This illustrates an important and previously un-
 203 explored feedback between marsh and river delta sediment accumulation.

204 The emergent effect of the interaction between marsh and clastic sedimentation is
 205 the decreased slope of the subaerial marsh window. The flattening within the marsh win-
 206 dow and accumulation of marsh proxy sediment here simultaneously created a 10% larger
 207 delta top (Figure 2a), but with a \sim 100% larger marsh window. Because the treatment
 208 experiment has smaller slopes from the shoreline to the top of the marsh window and
 209 the shoreline location changes only slightly (Figure 2d), the area from the top of the marsh
 210 window to the apex must be smaller in the treatment experiment (Figure 2d). Marshes

211 do not erode sediment from upstream to include within the marsh window, yet the lower
212 slopes of a marsh in dynamic equilibrium with its delta effectively “steal” clastic sed-
213 iment from higher elevations. For example, the area above the marsh accumulated 3 times
214 less clastic volume in the treatment experiment (Table 1). Instead, the remaining sed-
215 iment trapped on the delta top is sequestered in the marsh window, which accumulates
216 1.3 times more clastic volume (Table 1) than the control. While marsh deposition changes
217 the sediment balance between the marsh window and elevations above it, the clastic sed-
218 iment partitioning of the topset and foreset remains similar. Even so, the decreased slope
219 and associated feedbacks leads to variation in spatial clastic deposition in the treatment
220 experiment as compared to the control.

221 Decreased delta top slopes have previously been shown to alter delta morphology
222 and increase channelization (Parker et al., 1998). Decreased delta slopes are a function
223 of grain size and cohesion (Caldwell & Edmonds, 2014; Q. Li et al., 2017; Edmonds &
224 Slingerland, 2010), as well as a function of the ratio of water to sediment discharge (Whipple
225 et al., 1998; Powell et al., 2012; Wickert et al., 2013). Here we suggest a new mechanism
226 for lowering delta top slope: non-riverine sedimentation in the floodplain. The slope break
227 caused by marshes has been shown to influence avulsion locations (Ratliff et al., 2021).
228 Hence, this process matters for modern-day and ancient river deltas, which often sup-
229 port large swaths of marsh.

230 **4.2 Delta hypsometry**

231 Equilibrium hypsometry, or the elevation distribution on the delta top, shows en-
232 hanced areas of elevations near sea level where marsh sedimentation or similar processes
233 are present (Figure 2b). Using the ETOPO Global Relief Model (NOAA) in Google Earth
234 Engine, we explore this hypothesis for four large river deltas (Mississippi River Delta,
235 Ganges Brahmaputra Meghna Delta, Mekong River Delta, and Rio Grande River Delta).
236 Despite coarse resolution and systematic errors in this DEM (Minderhoud et al., 2019),
237 comparison at the vertical scale of several meters is appropriate (supporting informa-
238 tion section 3, Figure 2). Scaling by channel depth (for comparison across scales) reveals
239 the general hypsometry of these deltas (Figure 4).

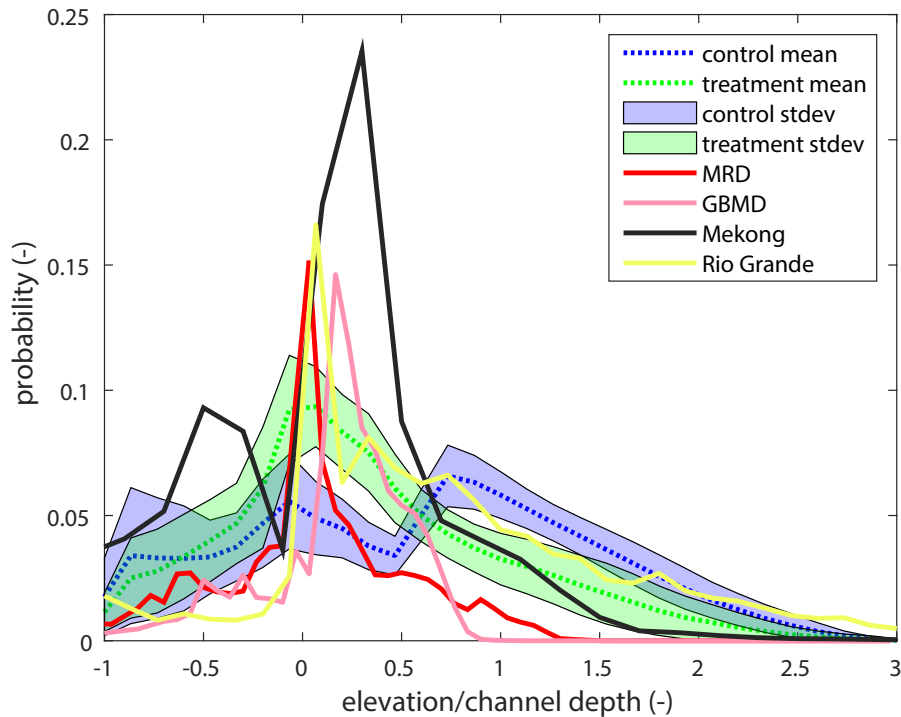


Figure 4: Hypsometry of the control and treatment experiments and four global deltas (Mississippi River [MRD], Ganges Brahmaputra Meghna [GBMD], Mekong, and Rio Grande). Elevation relative to sea level is scaled by the channel depth (x-axis) for comparison between field and experimental scale.

240 The treatment experiment and global deltas show a peak in elevations between 0
 241 to 0.5 channel depths relative to sea level (rsl), the domain of their marsh platforms. In
 242 both the treatment experiment and global deltas, >30% of all elevations between -1 and
 243 3 channel depths lie between 0 and 0.5 channel depths rsl, while the control experiment
 244 only has 15% of elevations here. Rather, the control experiment shows its peak around
 245 0.8 channel depths rsl due to increased slopes and associated reduced area near the shore-
 246 line. The marsh proxy organizes the treatment experiment's hypsometry to reflect the
 247 dominant hypsometric feature of delta systems and is an improvement over the control.
 248 At a minimum, this suggests that proxies for non-riverine, elevation-based coastal ac-
 249 cumulation can improve the fidelity of laboratory scale models. It also suggests that purely
 250 fluvial, lobe based delta deposition is insufficient to understand sedimentation in mod-
 251 ern deltas. While organic deposition is a reasonable control on these systems, tidal flat
 252 and barrier island reworking should also fundamentally influence delta hypsometry and
 253 sediment partitioning in similar ways, because they are also focused deposition near sea
 254 level. Succinctly, the coupling of marsh and river delta sediment deposition appears to
 255 be essential in shaping global deltas.

256 4.3 Implications

257 This work can be used to inform restoration and management plans on river deltas
 258 with significant marsh deposition. Successful restoration of deltaic wetlands hinges on

259 understanding delta hypsometry and the temporal and spatial clastic sediment deposi-
260 tion rates. While marsh sedimentation is relatively continuous in the marsh window, it
261 is important to note that this region accumulates primarily fluvial sediment. The extent
262 of this region is increased due to the feedbacks between the river and marsh. Given the
263 importance of channel-marsh interaction to the mass balance in the treatment experi-
264 ment and in the absence of other clastic sediment distribution mechanisms (e.g., tides
265 or storms), limiting channel-marsh interaction via leveeing could significantly alter the
266 feedbacks observed here.

267 Engineered marsh platforms must be consistent with how the wetland platform would
268 grow naturally (Paola et al., 2011). Modern deltas have elevation windows that matter
269 for habitability (higher elevation, fluvial ridges) and others that matter for storm surge
270 protection and biodiversity (lower elevation, marshes). The presence of marsh deposi-
271 tion on the shallow platforms created via river diversions (or other restoration methods)
272 will create mostly land at or near sea level. Thus, the probability distribution of eleva-
273 tions (Figure 2b) will eventually have implications for the extent of storm surges and sus-
274 ceptibility to drowning. Similarly, the change in coastal accumulation rates seen in the
275 treatment experiment has implications for the abiotic, fluvial deposit, particularly for
276 regions above the marsh (i.e., fluvial ridges). Fluvial ridges are typically the most pop-
277 ulated region of a river delta, existing solidly above the marsh. Since the interaction be-
278 tween rivers and marshes controls this area partitioning, it should be a significant con-
279 trol on modern deltas and any future river diversions created to support them.

280 5 Conclusion

281 We show that the addition of marsh proxy sedimentation in a delta experiment fun-
282 damentally alters the mass balance and hypsometry of the resulting delta. Specifically,
283 we find a new control on delta top slope: marsh accumulation. The decreased marsh win-
284 dowslope creates feedbacks that impact the spatial and temporal distribution of river-
285 ine sediment, leading to increased area near sea level. The interaction of river and marsh
286 sediment in the treatment experiment leads to a morphological signature more consis-
287 tent with modern-day river deltas than the control. Since marshes grow to keep pace with
288 relative sea level rise in the low-lying regions of the delta, they fundamentally flatten land
289 near the coast creating the vast marsh platforms seen globally. The lower slopes create
290 feedbacks with clastic sediment deposition patterns that will help to inform future restora-
291 tion plans, as these plans typically hinge on the successful distribution and retention of
292 riverine sediment.

293 Acknowledgments

294 The project was funded in part by an NSF grant (co PIs Kyle Straub; NSF EAR-
295 1848994 that funded Kyle Straub and Jose Silvestre’s time plus much of the experimen-
296 tal costs and John Shaw; NSF EAR-1848993 that funded John Shaw and Sam Zapp’s
297 time plus some of the experimental costs) and in part by the U.S. Geological Survey (funded
298 Kelly Sanks’ hourly work). We have no known conflicts of interest. We would like to thank
299 Dr. Eric Barefoot for his monumental help in automating the treatment experiment.

300 Open Research

301 Data and software that reproduce the results of this study are hosted in Zenodo
302 (<https://doi.org/10.5281/zenodo.5911147>) and Github ([https://github.com/kmsanks/
303 TDWB_19_2_MassBalance_Morphology](https://github.com/kmsanks/TDWB_19_2_MassBalance_Morphology)) repositories.

304 Data archiving of the raw experimental data is underway and will be available at
305 the “Tulane_Sediment_Dynamics_Stratigraphy_TSDS” project space: <https://sead2.ncsa>

306 .illinois.edu/spaces/5825f529e4b0f3dd19c8d93a (TDB-18-1 and TDWB-19-2-Surface-
 307 Processes) upon review. Note, this data is not needed to reproduce any results from the
 308 study, but may be of interest for other researchers. All data used in this study is archived
 309 in the Zenodo or Github repositories (see above).

310 References

- 311 Allen, J. (2000, July). Morphodynamics of Holocene salt marshes: a review sketch
 312 from the Atlantic and Southern North Sea coasts of Europe. *Quaternary Sci-*
 313 *ence Reviews*, 19(12), 1155–1231. doi: 10.1016/S0277-3791(99)00034-7
- 314 Baustian, J. J., Mendelssohn, I. A., & Hester, M. W. (2012). Vegetation’s impor-
 315 tance in regulating surface elevation in a coastal salt marsh facing elevated
 316 rates of sea level rise. *Global Change Biology*, 18(11), 3377–3382. Retrieved
 317 2021-12-29, from [https://onlinelibrary.wiley.com/doi/abs/10.1111/](https://onlinelibrary.wiley.com/doi/abs/10.1111/j.1365-2486.2012.02792.x)
 318 [j.1365-2486.2012.02792.x](https://onlinelibrary.wiley.com/doi/abs/10.1111/j.1365-2486.2012.02792.x) doi: 10.1111/j.1365-2486.2012.02792.x
- 319 Bohacs, K., & Suter, J. (1997, October). Sequence Stratigraphic Distribution
 320 of Coaly Rocks: Fundamental Controls and Paralic Examples. *AAPG*
 321 *Bulletin*, 81(10), 1612–1639. Retrieved 2021-06-14, from [https://](https://pubs.geoscienceworld.org/aapgbull/article-abstract/81/10/1612/39371/Sequence-Stratigraphic-Distribution-of-Coaly-Rocks)
 322 [pubs.geoscienceworld.org/aapgbull/article-abstract/81/10/1612/](https://pubs.geoscienceworld.org/aapgbull/article-abstract/81/10/1612/39371/Sequence-Stratigraphic-Distribution-of-Coaly-Rocks)
 323 [39371/Sequence-Stratigraphic-Distribution-of-Coaly-Rocks](https://pubs.geoscienceworld.org/aapgbull/article-abstract/81/10/1612/39371/Sequence-Stratigraphic-Distribution-of-Coaly-Rocks) doi:
 324 [10.1306/3B05C3FC-172A-11D7-8645000102C1865D](https://pubs.geoscienceworld.org/aapgbull/article-abstract/81/10/1612/39371/Sequence-Stratigraphic-Distribution-of-Coaly-Rocks)
- 325 Cahoon, D. R., Reed, D. J., & Day, J. W. (1995, October). Estimating shallow sub-
 326 sidence in microtidal salt marshes of the southeastern United States: Kaye and
 327 Barghoorn revisited. *Marine Geology*, 128(1-2), 1–9. Retrieved 2017-04-20,
 328 from <http://linkinghub.elsevier.com/retrieve/pii/002532279500087F>
 329 doi: 10.1016/0025-3227(95)00087-F
- 330 Caldwell, R. L., & Edmonds, D. A. (2014). The effects of sediment properties on
 331 deltaic processes and morphologies: A numerical modeling study. *Journal of*
 332 *Geophysical Research: Earth Surface*, 119(5), 961–982. Retrieved 2022-01-11,
 333 from <https://onlinelibrary.wiley.com/doi/abs/10.1002/2013JF002965>
 334 doi: 10.1002/2013JF002965
- 335 Chesnut, J., & Greb, S. F. (1992, January). Lowstand versus highstand eustatic
 336 models for peat preservation: The coal-bearing rocks of the Breathitt Group,
 337 Eastern Kentucky. *Geological Society of America, Abstracts with Programs;*
 338 *(United States)*, 24:7.
- 339 Edmonds, D. A., Hoyal, D. C. J. D., Sheets, B. A., & Slingerland, R. L. (2009, Au-
 340 gust). Predicting delta avulsions: Implications for coastal wetland restoration.
 341 *Geology*, 37(8), 759–762. doi: 10.1130/G25743A.1
- 342 Edmonds, D. A., & Slingerland, R. L. (2008). Stability of delta distributary net-
 343 works and their bifurcations. *Water Resources Research*, 44(9). Retrieved
 344 2021-06-14, from [https://agupubs.onlinelibrary.wiley.com/doi/abs/](https://agupubs.onlinelibrary.wiley.com/doi/abs/10.1029/2008WR006992)
 345 [10.1029/2008WR006992](https://agupubs.onlinelibrary.wiley.com/doi/abs/10.1029/2008WR006992) doi: 10.1029/2008WR006992
- 346 Edmonds, D. A., & Slingerland, R. L. (2010, February). Significant effect of sedi-
 347 ment cohesion on delta morphology. *Nature Geoscience*, 3(2), 105–109. doi: 10
 348 .1038/ngeo730
- 349 Ericson, J., Vorosmarty, C., Dingman, S., Ward, L., & Meybeck, M. (2006, Febru-
 350 ary). Effective sea-level rise and deltas: Causes of change and human dim-
 351 ension implications. *Global and Planetary Change*, 50(1-2), 63–82. Re-
 352 trieved 2017-04-20, from [http://linkinghub.elsevier.com/retrieve/pii/](http://linkinghub.elsevier.com/retrieve/pii/S0921818105001827)
 353 [S0921818105001827](http://linkinghub.elsevier.com/retrieve/pii/S0921818105001827) doi: 10.1016/j.gloplacha.2005.07.004
- 354 Esposito, C. R., Shen, Z., Törnqvist, T. E., Marshak, J., & White, C. (2017,
 355 July). Efficient retention of mud drives land building on the Mississippi
 356 Delta plain. *Earth Surface Dynamics*, 5(3), 387–397. Retrieved 2021-06-
 357 14, from <https://esurf.copernicus.org/articles/5/387/2017/> doi:
 358 [10.5194/esurf-5-387-2017](https://esurf.copernicus.org/articles/5/387/2017/)

- 359 Holmquist, J. R., Windham-Myers, L., Bliss, N., Crooks, S., Morris, J. T., Mego-
360 nical, J. P., ... Woodrey, M. (2018, June). Accuracy and Precision of Tidal
361 Wetland Soil Carbon Mapping in the Conterminous United States. *Scientific*
362 *Reports*, 8(1), 9478. Retrieved 2022-01-21, from [https://www.nature.com/](https://www.nature.com/articles/s41598-018-26948-7)
363 [articles/s41598-018-26948-7](https://www.nature.com/articles/s41598-018-26948-7) (Bandiera_abtest: a Cc.license_type: cc_by
364 Cg_type: Nature Research Journals Number: 1 Primary_atype: Research Pub-
365 lisher: Nature Publishing Group Subject_term: Carbon cycle;Climate-change
366 mitigation Subject_term_id: carbon-cycle;climate-change-mitigation) doi:
367 10.1038/s41598-018-26948-7
- 368 Hoyal, D. C. J. D., & Sheets, B. A. (2009). Morphodynamic evolution of experimen-
369 tal cohesive deltas. *Journal of Geophysical Research: Earth Surface*, 114(F2).
370 doi: 10.1029/2007JF000882
- 371 Kirwan, M. L., Guntenspergen, G. R., D'Alpaos, A., Morris, J. T., Mudd, S. M.,
372 & Temmerman, S. (2010, December). Limits on the adaptability of coastal
373 marshes to rising sea level: ecogeomorphic limits to wetland survival. *Geo-*
374 *physical Research Letters*, 37(23). Retrieved 2017-04-20, from [http://](http://doi.wiley.com/10.1029/2010GL045489)
375 doi.wiley.com/10.1029/2010GL045489 doi: 10.1029/2010GL045489
- 376 Kirwan, M. L., & Murray, A. B. (2007, April). A coupled geomorphic and eco-
377 logical model of tidal marsh evolution. *Proceedings of the National Academy of*
378 *Sciences*, 104(15), 6118–6122. Retrieved 2017-04-20, from [http://www.pnas](http://www.pnas.org/cgi/doi/10.1073/pnas.0700958104)
379 [.org/cgi/doi/10.1073/pnas.0700958104](http://www.pnas.org/cgi/doi/10.1073/pnas.0700958104) doi: 10.1073/pnas.0700958104
- 380 Li, Q., Benson, W. M., Harlan, M., Robichaux, P., Sha, X., Xu, K., & Straub, K. M.
381 (2017). Influence of Sediment Cohesion on Deltaic Morphodynamics and
382 Stratigraphy Over Basin-Filling Time Scales. *Journal of Geophysical Research:*
383 *Earth Surface*, 122(10), 1808–1826. doi: 10.1002/2017JF004216
- 384 Li, S., Wang, G., Deng, W., Hu, Y., & Hu, W. (2009, December). Influence of
385 hydrology process on wetland landscape pattern: A case study in the Yel-
386 low River Delta. *Ecological Engineering*, 35(12), 1719–1726. Retrieved
387 2021-08-22, from [https://www.sciencedirect.com/science/article/pii/](https://www.sciencedirect.com/science/article/pii/S0925857409002122)
388 [S0925857409002122](https://www.sciencedirect.com/science/article/pii/S0925857409002122) doi: 10.1016/j.ecoleng.2009.07.009
- 389 Minderhoud, P. S. J., Coumou, L., Erkens, G., Middelkoop, H., & Stouthamer, E.
390 (2019, August). Mekong delta much lower than previously assumed in sea-level
391 rise impact assessments. *Nature Communications*, 10(1), 3847. Retrieved
392 2021-06-08, from <https://www.nature.com/articles/s41467-019-11602-1>
393 doi: 10.1038/s41467-019-11602-1
- 394 Morris, J. T., Sundareshwar, P. V., Nietch, C. T., Kjerfve, B., & Cahoon, D. R.
395 (2002, October). Responses of Coastal Wetlands to Rising Sea Level. *Ecology*,
396 83(10), 2869–2877. doi: 10.1890/0012-9658
- 397 Nyman, J. A., Walters, R. J., Delaune, R. D., & Patrick, W. H. (2006, Septem-
398 ber). Marsh vertical accretion via vegetative growth. *Estuarine, Coastal*
399 *and Shelf Science*, 69(3), 370–380. Retrieved 2021-06-14, from [https://](https://www.sciencedirect.com/science/article/pii/S0272771406001843)
400 www.sciencedirect.com/science/article/pii/S0272771406001843 doi:
401 10.1016/j.ecss.2006.05.041
- 402 Paola, C., Straub, K., Mohrig, D., & Reinhardt, L. (2009, December). The
403 “unreasonable effectiveness” of stratigraphic and geomorphic experi-
404 ments. *Earth-Science Reviews*, 97(1), 1–43. Retrieved 2020-08-12, from
405 <http://www.sciencedirect.com/science/article/pii/S001282520900083X>
406 doi: 10.1016/j.earscirev.2009.05.003
- 407 Paola, C., Twilley, R. R., Edmonds, D. A., Kim, W., Mohrig, D., Parker, G., ...
408 Voller, V. R. (2011). Natural processes in delta restoration: application
409 to the Mississippi Delta. *Annual Review of Marine Science*, 3, 67–91. doi:
410 10.1146/annurev-marine-120709-142856
- 411 Parker, G., Paola, C., Whipple, K. X., & Mohrig, D. (1998, October). Alluvial Fans
412 Formed by Channelized Fluvial and Sheet Flow. I: Theory. *Journal of Hy-*
413 *draulic Engineering*, 124(10), 985–995. Retrieved 2021-10-12, from <https://>

- 414 ascelibrary.org/doi/abs/10.1061/(ASCE)0733-9429(1998)124:10(985)
415 doi: 10.1061/(ASCE)0733-9429(1998)124:10(985)
- 416 Powell, E. J., Kim, W., & Muto, T. (2012). Varying discharge controls on timescales
417 of autogenic storage and release processes in fluvio-deltaic environments: Tank
418 experiments. *Journal of Geophysical Research: Earth Surface*, 117(F2). Re-
419 trieved 2022-01-12, from [https://onlinelibrary.wiley.com/doi/abs/](https://onlinelibrary.wiley.com/doi/abs/10.1029/2011JF002097)
420 10.1029/2011JF002097 doi: 10.1029/2011JF002097
- 421 Ratliff, K. M., Hutton, E. W. H., & Murray, A. B. (2021, April). Modeling
422 long-term delta dynamics reveals persistent geometric river avulsion loca-
423 tions. *Earth and Planetary Science Letters*, 559, 116786. Retrieved 2021-
424 09-17, from [https://www.sciencedirect.com/science/article/pii/](https://www.sciencedirect.com/science/article/pii/S0012821X21000455)
425 S0012821X21000455 doi: 10.1016/j.epsl.2021.116786
- 426 Sanks, K. M., Shaw, J. B., & Naithani, K. (2020). Field-Based Estimate of the
427 Sediment Deficit in Coastal Louisiana. *Journal of Geophysical Research: Earth*
428 *Surface*, 125(8). doi: 10.1029/2019JF005389
- 429 Smart, J. S., & Moruzzi, V. L. (1971, January). *Quantitative Properties of Delta*
430 *Channel Networks* (Tech. Rep.). IBM Thomas J Watson Research Center,
431 Yorktown Heights, NY.
- 432 Straub, K. M., Paola, C., Mohrig, D., Wolinsky, M. A., & George, T. (2009, Septem-
433 ber). Compensational Stacking of Channelized Sedimentary Deposits. *Jour-
434 nal of Sedimentary Research*, 79(9), 673–688. Retrieved 2022-01-11, from
435 <https://doi.org/10.2110/jsr.2009.070> doi: 10.2110/jsr.2009.070
- 436 Whipple, K., Parker, G., Paola, C., & Mohrig, D. (1998, November). Channel
437 Dynamics, Sediment Transport, and the Slope of Alluvial Fans: Experimen-
438 tal Study. *The Journal of Geology*, 106(6), 677–694. Retrieved 2022-01-17,
439 from <https://www.journals.uchicago.edu/doi/10.1086/516053> doi:
440 10.1086/516053
- 441 Wickert, A. D., Martin, J. M., Tal, M., Kim, W., Sheets, B., & Paola, C. (2013).
442 River channel lateral mobility: metrics, time scales, and controls. *Journal of*
443 *Geophysical Research: Earth Surface*, 118(2), 396–412. Retrieved 2022-01-11,
444 from <https://onlinelibrary.wiley.com/doi/abs/10.1029/2012JF002386>
445 doi: 10.1029/2012JF002386